

Article

Mechanochemical Synthesis of Dolomite-Related Carbonates—Insight into the Effects of Various Parameters

Ting Jiang ¹, Chao Wang ¹, Min Chen ¹, Huimin Hu ², Junwei Huang ¹, Xiaofang Chen ¹ and Qiwu Zhang ^{1,*}

¹ School of Resources & Environmental Engineering, Wuhan University of Technology, Wuhan 430070, China; chen_min@whut.edu.cn (M.C.)

² State Environmental Protection Key Laboratory of Water Environmental Simulation and Pollution Control, South China Institute of Environmental Sciences, Ministry of Ecology and Environment, Guangzhou 510655, China; huimin_hu2022@163.com

* Correspondence: zhangqw@whut.edu.cn; Tel.: +86-177714900085

Abstract: The low-temperature formation of dolomite ($\text{CaMg}(\text{CO}_3)_2$) is undoubtedly a long and interesting geological problem, which has troubled many researchers for centuries to explore the formation of dolomite. Recently, efforts have been made by synthesizing dolomite analogues such as norsethite ($\text{BaMg}(\text{CO}_3)_2$), $\text{PbMg}(\text{CO}_3)_2$, with Ba and Pb to replace Ca and investigating their reaction pathways. In this study, we reported our efforts to synthesize dolomite-related complex carbonates by using the mechanical ball milling method as a new approach to control the solid–water ratio compared to the commonly used solution method. Two analogues of norsethite and $\text{PbMg}(\text{CO}_3)_2$ have been simply obtained even at stoichiometric molar ratio of Ba/Mg = 1:1 and Pb/Mg = 1:1 with various parameters examined; and product properties including morphology and phase compositions were investigated by a range of techniques, including XRD, SEM-EDS, and FTIR. Finally, we attempted to synthesize dolomite and compared the differences from the synthesis of analogues. In conclusion, we have synthesized norsethite and $\text{PbMg}(\text{CO}_3)_2$ in one step by the ball milling method, which greatly reduces the reaction time compared with the conventional solution method and may provide other choices for the formation of dolomite.



Citation: Jiang, T.; Wang, C.; Chen, M.; Hu, H.; Huang, J.; Chen, X.; Zhang, Q. Mechanochemical Synthesis of Dolomite-Related Carbonates—Insight into the Effects of Various Parameters. *Minerals* **2023**, *13*, 1359. <https://doi.org/10.3390/min13111359>

Academic Editors: Elsabe Kearsley and Alexander Mikhailovich Kalinkin

Received: 4 September 2023

Revised: 19 October 2023

Accepted: 19 October 2023

Published: 25 October 2023



Copyright: © 2023 by the authors. Licensee MDPI, Basel, Switzerland. This article is an open access article distributed under the terms and conditions of the Creative Commons Attribution (CC BY) license (<https://creativecommons.org/licenses/by/4.0/>).

Keywords: dolomite; norsethite; $\text{PbMg}(\text{CO}_3)_2$; mechanochemical; ionic radius

1. Introduction

Dolomite, as a common mineral in nature, has a wide range of applications in the chemical industry, metallurgy and construction; however, its formation has puzzled researchers for centuries. It was first discovered by the French mineralogist and chemist Deodat Gratet de Dolomieu in the 18th century in the dolomite mountains of northern Italy [1,2]. In the following two hundred years, scientists conducted various syntheses of dolomite in the laboratory, without successful reports at temperatures below 100 °C [3,4]. In a classic experiment, Land placed magnesium calcite in a Mg^{2+} -rich solution for 32 years and could not successfully obtain the dolomite phase [5], so the low-temperature formation of dolomite has certainly become an interesting and long-standing mineralogical problem [6]. Although dolomite is a thermodynamically stable phase, more stable than magnesium calcite in seawater at surface temperature, seawater is supersaturated with respect to dolomite and not deposited in modern marine environments [7,8]. On the other hand, the presence of large amounts of dolomite indicates that there were significant amounts of dolomite precipitation in geological history [9–11]. This interesting phenomenon prompted researchers to take a keen interest in the question of “how dolomite was produced in the past”. Investigation of the formation of dolomite can help us to better understand the geographic variations in the past, and to consider the subsequent application of dolomite in different fields [12,13]. Due to the failure of the above experiments, a large number of hypotheses have been proposed to understand possible reasons for the difficult formation of dolomite: mainly including

the strong hydration of Mg^{2+} , the obstruction of sulfate, the ordering process of cations, the lower supersaturation and the lack of nucleation sites [14].

Faced with the difficulty of dolomite formation at room temperature and pressure, researchers have focused their attention on the study of dolomite analogues. Unlike dolomite, norsethite and $PbMg(CO_3)_2$ can be easily synthesized artificially in the laboratory [15]. The first synthesis of norsethite under laboratory conditions was at 500 °C [16]. Subsequently, Lippmann reported the synthesis of norsethite at room temperature for the first time [17]. Pimentel and Pina also tried to precipitate norsethite directly at room temperature, and they concluded that the formation of norsethite was achieved by a relatively complex solution-mediated maturation process [18,19]. Zhang synthesized norsethite and $PbMg(CO_3)_2$ by the carbon dioxide gas diffusion method at room temperature and found the initial Mg/Ba ratio a key factor [20]. On the other hand, the precipitation of $PbMg(CO_3)_2$ is always a multi-step precipitation process, irrespective of the Mg/Pb ratio range [19].

The mechanochemical method refers to the application of mechanical energy by ball milling to condensed substances such as solids and liquids by means of shear, abrasion, impact and extrusion to induce changes in their structure and physicochemical properties and to induce chemical reactions [21,22]. Considering the great amount of attention given to the strong hydration of Mg^{2+} , and the effect of ball milling on the syntheses of dolomite analogues and even proto-dolomite at room temperature and pressure confirmed by Longo [23], Longo pointed out that ball milling is very promising for obtaining dolomite and its analogs, but unfortunately there are no plots showing that they obtained dolomite and dolomite-like samples with super diffractive structural lines, and similarly attempts have been made to obtain dolomite by milling mixtures of magnesite and calcite, where they again did not obtain dolomite with an ordered structure, but only samples similar to the dolomite structure [24]. The X-ray diffraction pattern of the dolomite produced is similar to that of the protodolomite found in nature in that the diffraction lines are broad and show none of the diffraction lines characteristic of ordered dolomite. In order to further understand and answer the dolomite question, we have attempted to synthesize dolomite analogs and dolomite by mechanical ball milling. We compared in detail the differences between ball milling and solution operation in the syntheses of dolomite analogues, and even dolomite, to examine the effect of the solid–liquid ratio, and therefore Mg^{2+} hydration, as an attempt to answer, at least partially in a different aspect, the dolomite question [23].

Therefore, in this study, mechanical ball milling was used to synthesize dolomite analogs or even dolomite under normal temperature and pressure conditions, as well as to investigate the effect of Mg^{2+} hydration during dolomite formation and the different syntheses of different dolomite analogs by regulating the amount of water. Specifically, a series of parameters such as ball milling conditions (speeds or time) and amount of water added were used as factors in the investigation of the synthesis process of norsethite/ $PbMg(CO_3)_2$, to provide a new approach into the formation of dolomite-related carbonates.

2. Experimental Section

2.1. Material Preparation

All the used chemicals, magnesium chloride hexahydrate ($MgCl_2 \cdot 6H_2O$), barium chloride ($BaCl_2 \cdot 2H_2O$), lead chloride ($PbCl_2$), lead nitrate ($Pb(NO_3)_2$), barium carbonate ($BaCO_3$), calcium chloride dihydrate ($CaCl_2 \cdot 2H_2O$), and sodium carbonate (Na_2CO_3), were purchased from Sinopharm Chemical Reagent Co., Ltd. (Shanghai, China). All solutions were configured with deionized (DI) water produced by Milli-Q Direct 8/16 (18.2 MΩ cm) purification system.

$BaCl_2 \cdot 2H_2O/PbCl_2/CaCl_2 \cdot 2H_2O$, $MgCl_2 \cdot 6H_2O$ and Na_2CO_3 with a total mass of 2 g in a molar ratio of 1:1:2 were placed in a ball mill pot with a total volume of 45 cm³ equipped with seven ZrO_2 balls of 15 mm diameter for ball milling. We also put a total mass of 2 g of sample at the same proportion into 200 mL of deionized water to stir for the same time as a comparison test. The ball mill reaction was carried out at different milling speeds and milling times. Subsequently the ball-milled samples were taken out and stored

in a sealed bag. Washing to move the soluble salts including product NaCl was conducted by dispersing 0.1 g of the sample and stirring in 50 mL of deionized water for 5 min. The recovered samples after water washing were finally dried (50 °C—2 h) for characterization. To investigate the effect of Mg²⁺ hydration on formation, different amounts of water were added to the milling process. Finally, different raw materials such as BaCO₃, PbCl₂ and PbNO₃ were used to investigate the effect of solubility for the formation reactions.

2.2. Sample Characterization

The phase compositions and crystal structures of samples were identified by an X-ray diffractometer (XRD, D-MAX, Rigaku, Japan) using CuK α radiation ($\lambda = 1.5403 \text{ \AA}$) over the 2θ range of $10^\circ\text{--}70^\circ$ with a step size of 0.02° . FT-IR analyses were performed with the spectra in the transmittance mode recorded in the range of $400\text{--}4000 \text{ cm}^{-1}$ at a resolution of 4 cm^{-1} using the KBr method on a Nicolet6700 spectrometer (Thermo Fisher Scientific, Waltham, MA, USA). The surface morphologies of samples were observed using scanning electron microscopy (SEM, Phenom, Thermo scientific, USA). Thermal analysis of samples was performed by using a thermal analyzer system (STA449F3, NETZSCH, Bruker, Germany) from room temperature to 800 °C at a heating speed of $10 \text{ }^\circ\text{C}/\text{min}$ in nitrogen using 10 mg of each sample.

3. Results and Discussion

3.1. Syntheses of Dolomite and Its Analogues

Figure 1 shows the comparison between two methods of solution and ball milling with starting samples of BaCl₂•2H₂O, MgCl₂•6H₂O and Na₂CO₃ at a molar ratio of 1:1:2. Two patterns of the product phases from solution synthesis and mechanochemical ball milling were largely different. The results of the solution synthesis (the blue line in Figure 1) were mainly the phase of BaCO₃ together with BaMg(CO₃)₂. Surprisingly, after ball milling at 400 rpm for 1 h, the peaks in the pattern (The red line in Figure 1) were characteristic of BaMg(CO₃)₂, without observable peaks of BaCO₃. This proves the feasibility of ball milling in the synthesis process of dolomite analogues. In the process of solution agitation with a large amount of water, solubility would be a key factor and the difference in the solubility of Ba carbonate and Mg carbonate works as a barrier for homogeneous precipitation to form Ba and Mg bicarbonate. This is the reason why Ba carbonate was observed as the main phase from solution agitation.

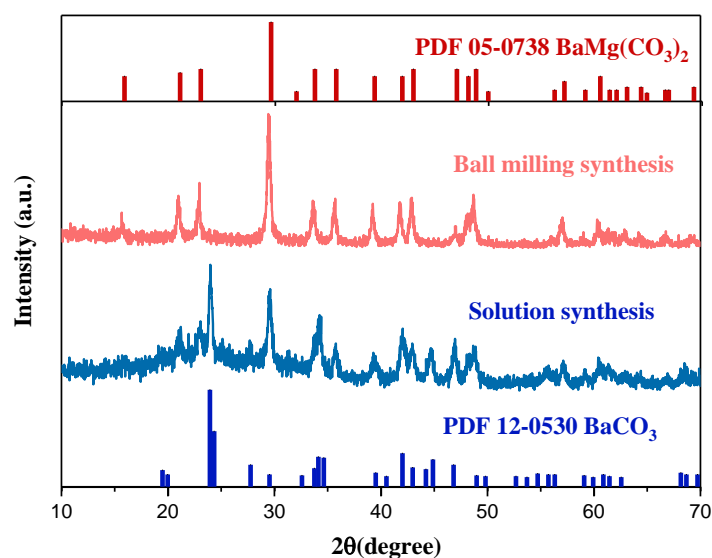


Figure 1. XRD patterns of the synthetic samples obtained for a 1 h operation (conditions: solution time:1 h, solid–liquid ratio:1:100; ball milling speed: 400 rpm and ball milling time: 1 h).

To examine the effect of ball milling operation on facilitating the phase formation of norsethite, the operation parameters, milling speed and milling time, were varied and XRD patterns obtained under different conditions are shown in Figure 2. It can be seen that the pure norsethite phase cannot be obtained at low rotational speeds (300 rpm for 1 h) and short times (400 rpm for 0.5 h), with BaCO_3 as the intermediate phase to $\text{BaMg}(\text{CO}_3)_2$. Pure norsethite without BaCO_3 has been synthesized at 400 rpm for 1 h, confirming that mechanical ball milling is beneficial for the synthesis of norsethite, resulting in a pure phase of norsethite with milling time or running speed over certain parameters. Ball milling provides a new approach for the synthesis of dolomite analogs, and may help to overcome the difficulty of dolomite phase formation at low temperatures. The reason why mechanochemical ball milling can facilitate the formation of the norsethite phase is that the action of mechanical forces such as shearing and crushing can in general reduce the particle size of reactants, break the internal chemical bond, destroy the crystal structure and expose the new chemical reaction interface, so as to promote the occurrence of chemical reactions that are difficult to initiate under normal conditions. More importantly, ball milling could allow operation at a very high solid–liquid ratio as well as a purely dry state, i.e., with a small amount of solvent to overcome the solubility problem in solution operations with a large amount of water.

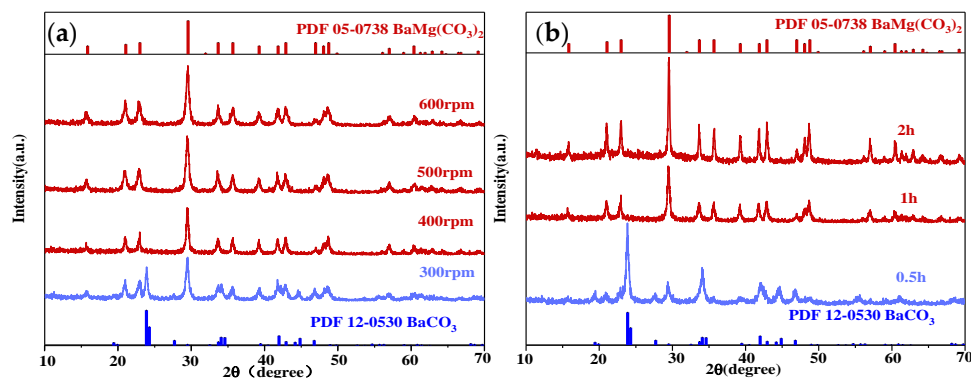


Figure 2. (a) XRD patterns of synthetic norsethite at different speeds (300 rpm, 400 rpm, 500 rpm and 600 rpm) at 1 h; (b) at different times (0.5 h, 1 h and 2 h) at 400 rpm.

Since Mg^{2+} ions have a strong hydration capacity, investigation of the effect of water quantity as an essential factor is conducted and Figure 3a shows the XRD patterns of the samples prepared with different amounts of water. XRD patterns of the samples had both phases of $\text{BaMg}(\text{CO}_3)_2$ and BaCO_3 when water was added at 0.5 mL and 1 mL. A noteworthy phenomenon is the occurrence of a pure phase of $\text{BaMg}(\text{CO}_3)_2$ in the milled sample, without BaCO_3 , when the added water volume was increased to 1.5 and 2 mL. Mechanochemical reactions are generally induced by dry milling, for example, solid particles together. The starting samples of Ba and Mg hydrated salts combine into a strongly agglomerated state, so a certain amount of water is needed to disperse the agglomerates. When 0.5 mL and 1 mL of water was added, the sample was not evenly dispersed during the ball milling process, so the reaction could not proceed smoothly. Subsequent water washing of the agglomerates gave a product with both phases of norsethite and the intermediate phase of Ba carbonate. More than 1.5 mL of deionized water in the reaction system ensures that the sample is well dispersed to allow the reaction to occur efficiently.

TG analysis was also performed to investigate the thermal behavior of the ball-milled norsethite samples with different amounts of water added after washing and drying. Figure 3b shows the TG data before 800 °C. The reaction process is as follows: Equation (1). The mass loss before 300 °C is considered to be the loss of crystalline adsorbed in the sample, while the weight loss at approximately 600 °C is considered to be the decomposition of $\text{BaMg}(\text{CO}_3)_2$ into CO_2 , MgO and BaCO_3 . The theoretical CO_2 release at this point is calculated to be 15.65% of the total mass. In addition, we can see that under different

conditions of applied water, the weight loss of crystalline water and adsorbed water below 300 °C is different. Combined with Figure 3a, we consider that the mass loss at the addition of 0.5 and 1 mL of water is less than at the addition of 1.5 and 2 mL of water because the pure phase of $\text{BaMg}(\text{CO}_3)_2$ was not obtained and the reaction did not occur exactly according to the molar ratio, resulting in some of the magnesium-containing salts being dissolved and carried away in the water, and so there was a smaller loss of mass as compared to that of the pure phase of orthoclase feldspar obtained at 1.5 and 2 mL [25]. Therefore, it is concluded by TG analysis that the norsethite and $\text{PbMg}(\text{CO}_3)_2$ samples synthesized by mechanical ball milling under certain conditions contain some crystalline water, mainly from the strong hydration of Mg^{2+} . This implied that the high energy barrier of dehydration of Mg^{2+} may not be the key reason to impede dolomite precipitation under low-temperature conditions [26]. A reasonable explanation is that Ba^{2+} , with a larger ionic radius, can more easily accommodate the incompletely dehydrated Mg^{2+} and establish the binding of Mg^{2+} to the surface carbonate to give $\text{BaMg}(\text{CO}_3)_2$ [27].

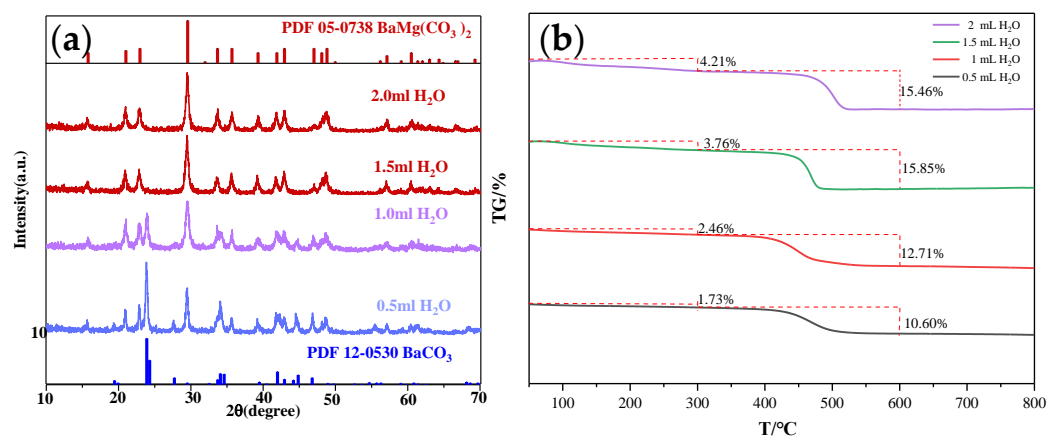
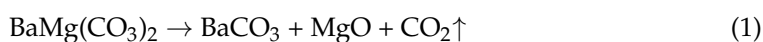


Figure 3. (a) XRD patterns of synthetic norsethite with different amounts of water added (0.5 mL, 1 mL, 1.5 mL and 2 mL); (b) thermogravimetric analysis of synthetic norsethite with different amounts of water added (0.5 mL, 1 mL, 1.5 mL and 2 mL) (conditions: ball milling speed: 400 rpm; ball milling time: 1 h).



In the previous experiments, the effects of ball milling speed, ball milling time and water volume were examined on norsethite synthesis, from which Ba carbonate as the intermediate phase was observed as a barrier to the formation of norsethite. In order to further understand and improve the formation process of norsethite, the effects of BaCO_3 the sample at three different states (chemical reagent without pretreatment; chemical reagent after ball milling activation; newly generated one from the reaction between Ba chloride and Na carbonate) as starting samples were investigated to compare its reactivity on synthesizing the norsethite phase by further co-milling with $\text{MgCl}_2 \cdot 6\text{H}_2\text{O}$ and Na_2CO_3 , respectively. Figure 4 shows the XRD patterns of the three ball-milled samples. When using chemical reagent BaCO_3 without activation by ball milling, peaks of BaCO_3 remained in the XRD pattern without observable new peaks of other phases including target norsethite, indicating the difficulty of the formation reaction with this very stable BaCO_3 sample. However, the synthesis product of $\text{BaMg}(\text{CO}_3)_2$ was successfully obtained when the newly generated BaCO_3 (400 r—1 h) and chemical reagent BaCO_3 activated by ball milling were used as starting materials. It is understood that for the formation process of norsethite, it is possible to incorporate Mg composition into the BaCO_3 structure in active states resulting from previous operations. Although some difficulties in synthesizing the norsethite phase do exist due to the easy appearance of Ba carbonate, milling operation could overcome this difficulty by facilitating the formation of the target product.

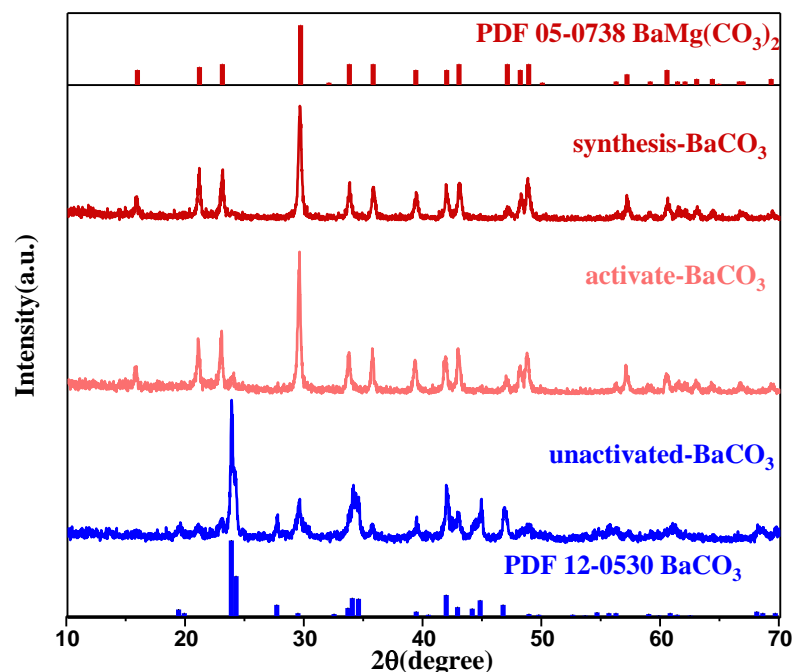


Figure 4. XRD patterns of synthetic norsethite from barium carbonate obtained under different conditions (synthesis conditions: ball milling speed 400 rpm and ball milling time 1 h).

Similar to norsethite, another dolomite analogue of $\text{PbMg}(\text{CO}_3)_2$ has been widely studied to explore the dolomite phenomenon. The possibility of synthesizing $\text{PbMg}(\text{CO}_3)_2$ was further examined in this study by using the same ball milling conditions as well as a solution method for comparison. With easily soluble Pb nitrate and partially soluble Pb chloride separately as starting samples, four samples from both milling operation and solution agitation were obtained, with the results shown in Figure 5. Under the conditions of PbCl_2 , $\text{MgCl}_2 \cdot 6\text{H}_2\text{O}$ and Na_2CO_3 as raw materials, there is a significant difference between the products formed by the solution and ball milling, with the former still dominated by the starting PbCl_2 phase and the latter by the newly generated $\text{Pb}_3(\text{CO}_3)_2(\text{OH})_2$, to which the formation of $\text{PbMg}(\text{CO}_3)_2$ was also confirmed as a minor phase. Compared with BaCl_2 of high solubility, the low solubility of PbCl_2 worked as a high barrier to the carbonation for agitation to overcome in order to form the dolomite analogue phase. Ball milling could activate it to give basic Pb carbonate as the main phase, but not reaching the final phase of $\text{PbMg}(\text{CO}_3)_2$. When the more soluble $\text{Pb}(\text{NO}_3)_2$ was used to replace PbCl_2 in both ball milling and solution agitation again, the $\text{Pb}_3(\text{CO}_3)_2(\text{OH})_2$ phase was obtained, this time even from solution agitation, indicating that it is easier to use soluble Pb nitrate for its carbonation with Na carbonate. However, even with $\text{Pb}(\text{NO}_3)_2$ as a raw material, milling operation has to be used to avoid this intermediate phase of $\text{Pb}_3(\text{CO}_3)_2(\text{OH})_2$ and to obtain the target phase of pure $\text{PbMg}(\text{CO}_3)_2$. Therefore, the apparent differences in the syntheses of the Pb-Mg dolomite analogue between two lead salts (PbNO_3 and PbCl_2) as raw materials under the same conditions indicated that the solubility of the starting samples plays an important role in obtaining the target product, supported by the large difference between the two salts with 54.3 g (PbNO_3) to 1 g (PbCl_2) per 100 mL water, respectively [28]. From the above results, we believe that many parameters may have a significant influence on the formation of the dolomite analogue, as well as dolomite itself, such as the atomic radii of the A-site elements [29,30], the solubility of the raw materials used, and the methods used of solution agitation alone or ball milling as an activating aid.

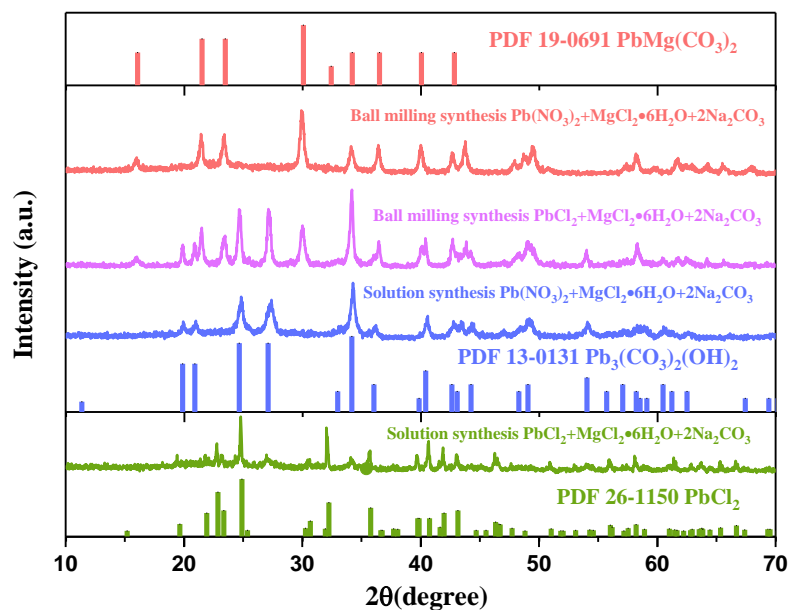


Figure 5. XRD patterns of synthetic $\text{PbMg}(\text{CO}_3)_2$ under different conditions (conditions: ball milling speed 400 rpm and ball milling time 1 h).

The functional groups of norsethite and $\text{PbMg}(\text{CO}_3)_2$ synthesized under solution agitation and ball milling by Fourier-transform infrared spectroscopy (FTIR) were examined, with results shown in Figure 6. According to the results in Figure 1, BaCO_3 and norsethite are found under solution agitation. Therefore, the absorption peaks of norsethite and BaCO_3 synthesized by solution agitation appear at 3422 cm^{-1} , 2454 cm^{-1} , 1812 cm^{-1} , 1751 cm^{-1} , 1452 cm^{-1} , 1117 cm^{-1} , 1059 cm^{-1} , 880 cm^{-1} , 857 cm^{-1} and 694 cm^{-1} , among which the absorption peaks at 1117 cm^{-1} , 880 cm^{-1} , 1479 cm^{-1} , 702 cm^{-1} and 1812 cm^{-1} correspond to the V1 (symmetric stretching vibration), V2 (out-of-plane bending vibration), V3 (antisymmetric stretching vibration), V4 (in-plane bending vibration), and V1 + V3 and V1 + V4 characteristic absorption peaks of the CO_3^{2-} of norsethite [31]. Meanwhile, the absorption peaks of BaCO_3 can also be observed at 857 cm^{-1} , 693 cm^{-1} , 1059 cm^{-1} , 1452 cm^{-1} , 1751 cm^{-1} and 2452 cm^{-1} . Notably, the difference in CO_3^{2-} between the two is extremely pronounced, with the pure phase of norsethite synthesized by ball milling showing a sharper peak than the carbonate product obtained under solution stirring agitation, which suggests a change in the environment in which the CO_3^{2-} is located ($\text{BaMg}(\text{CO}_3)_2$ — 1479 cm^{-1} VS. BaCO_3 — 1452 cm^{-1}). However, the absorption peaks of norsethite synthesized by ball-milled synthetic samples were present at only 1117 cm^{-1} , 880 cm^{-1} , 1479 cm^{-1} , 702 cm^{-1} , and 1812 cm^{-1} corresponding to the CO_3^{2-} of norsethite. No characteristic absorption peaks of BaCO_3 were observed, further indicating that the ball-milled sample did not contain the intermediate phase of BaCO_3 .

Similarly, for the synthetic $\text{PbMg}(\text{CO}_3)_2$ samples, the peaks obtained under solution conditions at 3438 , 1735 , 1045 , 1409 , and 681 cm^{-1} can be attributed to OH stretching vibration, CO_3 v3 vibration, OH flattening, CO_3 v3 vibration, and CO_3 v4 vibration, indicating the presence of CO_3^{2-} and OH^- in $\text{Pb}_3(\text{CO}_3)_2(\text{OH})_2$, while the IR absorption peaks obtained for the ball-milled synthetic samples are only those of $\text{PbMg}(\text{CO}_3)_2$, with peaks at 870 , 1437 , 707 , and 1797 cm^{-1} corresponding to CO_3 V2 (out-of-plane bending vibration), CO_3 V3 (antisymmetric stretching vibration), CO_3 V4 (in-plane bending vibration), CO_3 V1 + V3 and V1 + V4 characteristic absorption peaks of $\text{PbMg}(\text{CO}_3)_2$, respectively [28]. Finally, the differences in samples under ball milling and solution agitation syntheses were further illustrated and confirmed by the FTIR.

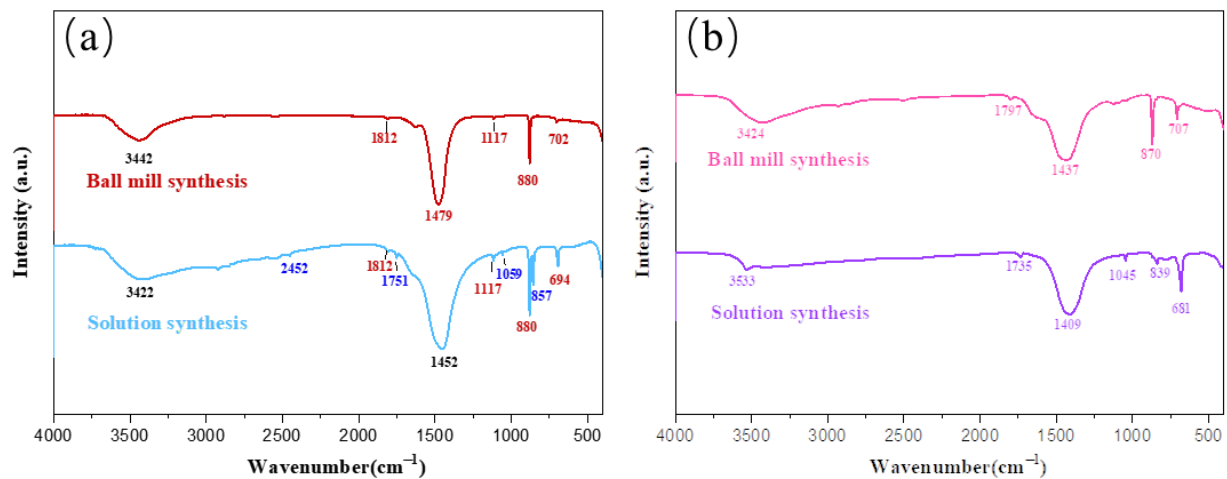


Figure 6. FTIR patterns of the synthesized norsethite (a) and $\text{PbMg}(\text{CO}_3)_2$ (b) under different conditions.

Figures 7 and 8 show the FESEM plots and EDS of the synthesized norsethite and $\text{PbMg}(\text{CO}_3)_2$ by ball milling at 400 rpm for 1 h. From Figures 7a–c and 8a–c, it can be observed that the products are monodisperse homogeneous crystals with small crystal sizes. Synthetic samples are relatively homogeneous, with particle sizes in the range of 10–100 nm. Additionally, comparing Figures 7e and 8e, Ba/Mg in the product is close to 1:1 in the synthesis of norsethite; and Pb/Mg is also close to 1:1 in the synthesis of $\text{PbMg}(\text{CO}_3)_2$. Therefore, it was proved that the samples obtained by ball milling were pure phases of norsethite and $\text{PbMg}(\text{CO}_3)_2$, respectively, and did not contain much intermediate-phase BaCO_3 and $\text{Pb}_3(\text{CO}_3)_2(\text{OH})_2$.

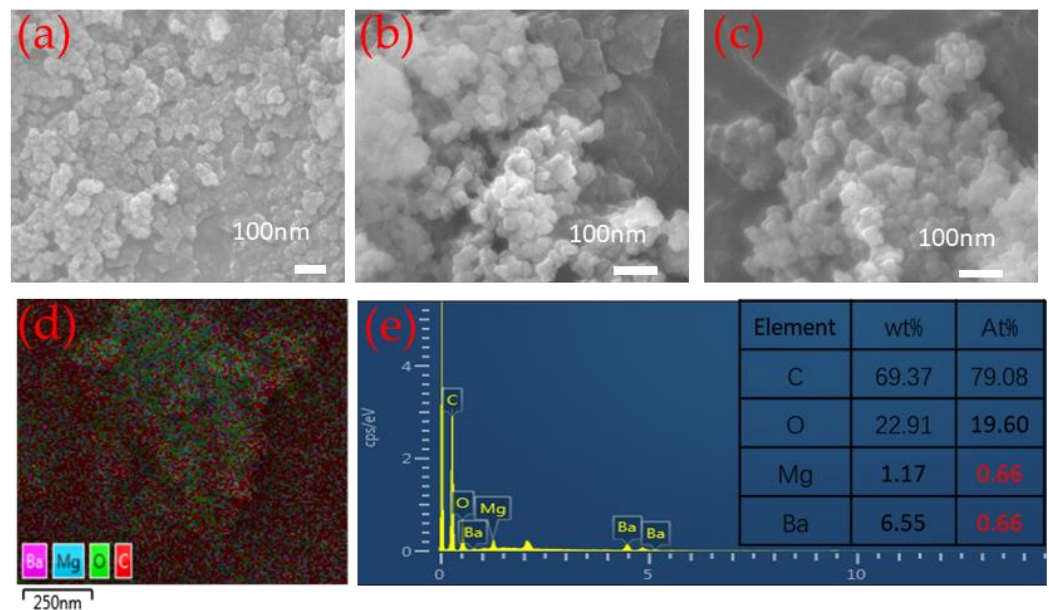


Figure 7. The SEM analysis and EDS element analysis of synthetic norsethite.

After a series of experiments on exploring suitable conditions for the synthesis of dolomite analogs, the following effort lies in an exploration for possible synthesis of the dolomite phase, namely using $\text{CaCl}_2 \cdot 2\text{H}_2\text{O}$, $\text{MgCl}_2 \cdot 6\text{H}_2\text{O}$ and Na_2CO_3 as raw materials under ball milling and solution agitation, respectively. The results are shown in Figure 9. The product under solution agitation was clearly only CaCO_3 pure phase, which similar to the result of the BaCO_3 phase shown in Figure 1. Compared with the relatively high solubility of Mg carbonate, the very low solubility of both Ba and Ca carbonates was the main reason for their precipitation on solution agitation. It is worthy of notice that under

ball milling conditions, a different pattern was observed, with a significant shift in the (1 0 4) peak of the synthesized sample, indicating the entry of Mg^{2+} into the structure of calcium carbonate. Although the characteristic diffraction peaks of dolomite were not observed and the peak intensity was very poor in general, all the peaks in the pattern were basically found to match that of the dolomite phase, suggesting that ball milling may help to increase the chance of dolomite synthesis, even if not a pure phase, as the reported analogues in Figures 1 and 5. Even with the aid of ball milling, it is still more difficult to obtain dolomite $CaMg(CO_3)_2$ than $BaMg(CO_3)_2$, or $PbMg(CO_3)_2$. Much expectation may be put on the chance to synthesize the real dolomite phase by the ball milling method through regulating parameters to find out suitable conditions, which is under planning.

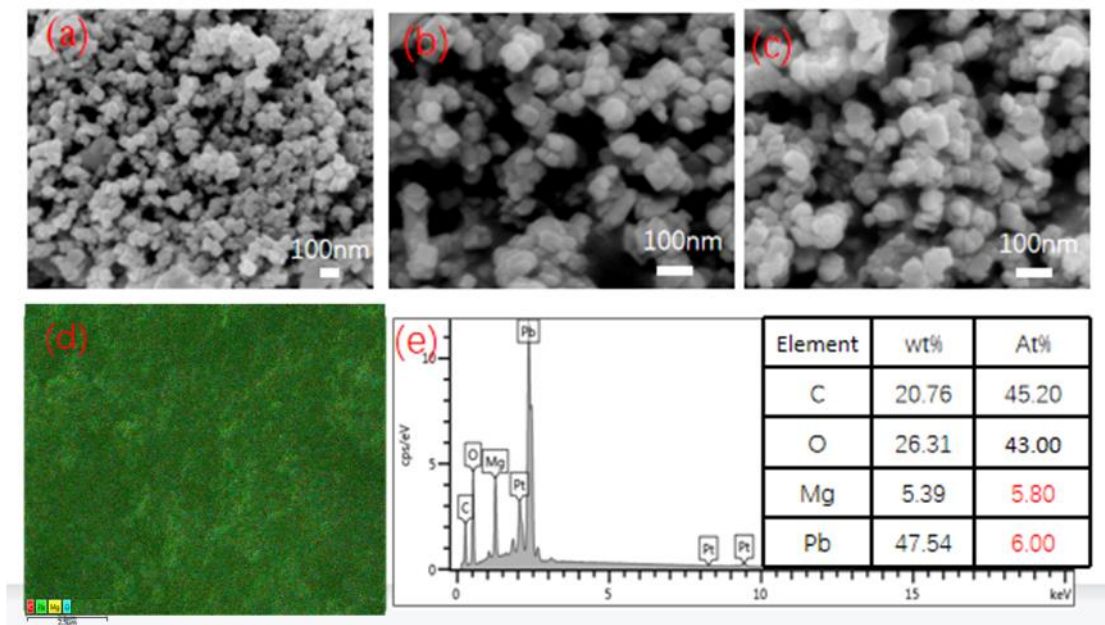


Figure 8. The SEM analysis and EDS element analysis of synthetic $PbMg(CO_3)_2$.

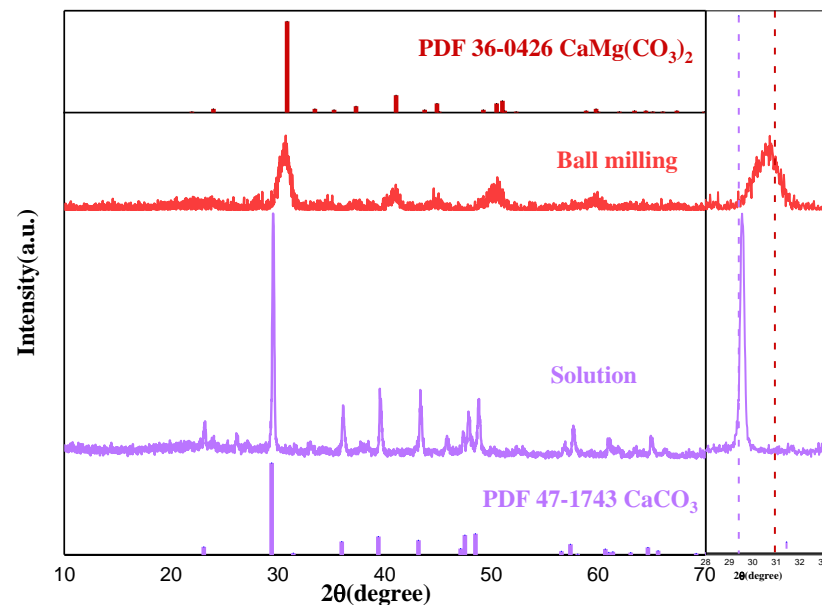


Figure 9. XRD patterns of the synthetic dolomite (conditions: ball milling speed 400 rpm and ball milling time 1 h).

Our group have performed studies on applying carbonates, particularly minerals to deal with wastewater treatment, and found out clear different features from traditional CaO neutralization [32–35]. Considering the difficulty in using mineral calcite to remove Mn^{2+} from wastewater, synthesized norsethite and calcium-magnesium carbonate for heavy metal manganese removal experiments were used at an exact molar ratio of 1:1 Mn^{2+} to CO_3^{2-} , i.e., the minimum amount of carbonate sample. Final results are shown in Table 1. It can be seen that the norsethite sample demonstrated a poor effect on Mn^{2+} removal, probably due to the very stable structure, which does not offer enough active sites for the combination of Mn^{2+} with carbonate anions. On the other hand, the calcium-magnesium carbonate sample gave quite a high removal efficiency of 70% of Mn^{2+} , suggesting a possible application in heavy metal treatment from wastewater of the synthesized carbonate with a not pure dolomite structure. The problem of dolomite synthesis and possible reactivity with heavy metal ions will be further investigated in future work, which also offers a potential application for dolomite in industry.

Table 1. Efficiency of Mn^{2+} removal by the prepared norsethite and $(\text{Ca},\text{Mg})\text{CO}_3$.

Sample	Mn^{2+} Removal Percentage
$\text{BaMg}(\text{CO}_3)_2$	17.49%
$(\text{Ca}, \text{Mg})\text{CO}_3$	70.03%

3.2. Mechanisms Discussion

Among the explorations into synthesizing norsethite, $\text{PbMg}(\text{CO}_3)_2$ and dolomite, the difference in the synthesis process of the three samples was compared, and it has been found that there are many factors to influence the formation of dolomite, so it is very important to understand the structures of dolomite and its analogues to explain the dolomite problem. The structure of dolomite is alternately arranged by Ca^{2+} and Mg^{2+} along its crystallography c-axis direction every other layer of CO_3^{2-} , with cation occupation in a completely ordered state. Ca^{2+} with a larger radius occupies the A-site, and Mg^{2+} with a smaller radius occupies B-site. The appearance of superstructure diffraction lines ($h\ 0\ l$) and $(0\ k\ l)$ in the spectrum by X-ray diffractograms (where l is an odd number) marks the generation of ordered structures in dolomite. The structure of dolomite is shown in Figure 10. Dolomite analogues have a similar structure to dolomite, as shown in Figure 11 [36]. It is known that the structure of norsethite ($\text{BaMg}(\text{CO}_3)_2$)/ $\text{PbMg}(\text{CO}_3)_2$ changes from that of the normal dolomite due to the larger ions at the A-site [37]. Specifically, since the ionic radius of Ba^{2+} / Pb^{2+} is larger than that of Ca^{2+} , the coordination number of its A-site cations has been changed from the original 6 coordination number of Ca^{2+} to the 12 coordination number of Ba^{2+} / Pb^{2+} ($6 + 6$), with six nearer oxygen atoms and six more distant oxygen atoms to form two octahedra with different Ba-O bond lengths, respectively. Therefore, it is worth noting that norsethite is not considered to be a complete isotype of dolomite, but a subtype of dolomite [38]. Similarly, $\text{PbMg}(\text{CO}_3)_2$ with a larger ionic radii belongs to the subtype of dolomite. The difference in A-site ions radius is also the reason for the difference in synthesis difficulty between the analogues of norsethite, $\text{PbMg}(\text{CO}_3)_2$ and dolomite itself. A larger A-site ions radius can provide more space to accommodate incompletely dehydrated Mg^{2+} , which makes it easier to form dolomite analogues. However, the obtained results suggest that milling operation may work in a beneficial way to improve the capacity of Ca^{2+} to incorporate the incompletely hydrated Mg^{2+} into the structure and suitable conditions require further detailed investigations.

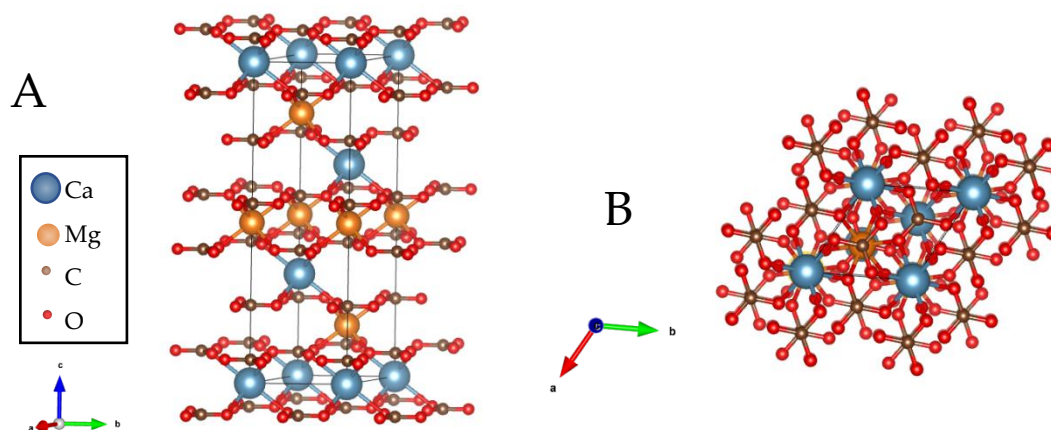


Figure 10. Side view (A) and top view (B) of the optimized unit cell of $\text{CaMg}(\text{CO}_3)_2$. Ca, Mg, C, and O are given in blue, orange, gray, and red, respectively.

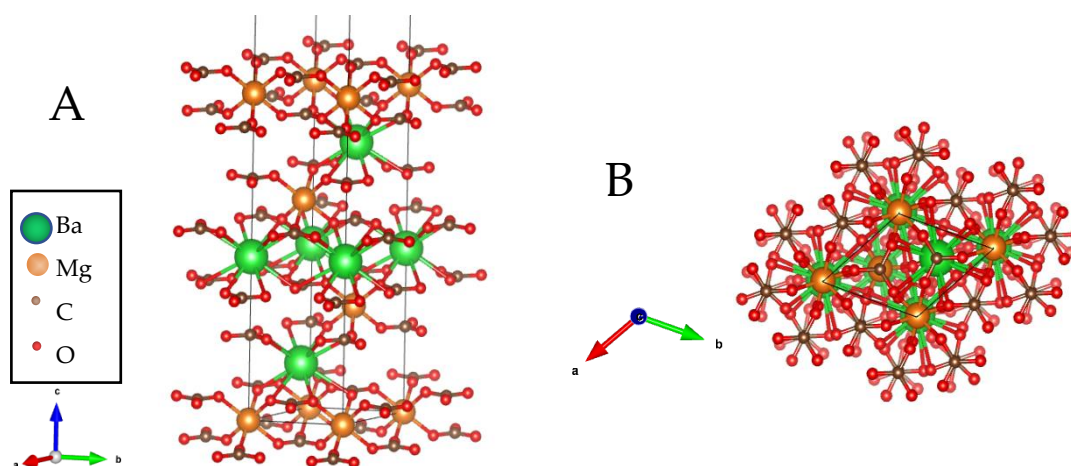


Figure 11. Side view (A) and top view (B) of the optimized unit cell of $\text{BaMg}(\text{CO}_3)_2$. Ba, Mg, C, and O are given in green, orange, gray, and red, respectively.

4. Conclusions

In this paper, norsethite and $\text{PbMg}(\text{CO}_3)_2$ were synthesized in one step under $\text{Ba}/\text{Mg} = 1:1$ and $\text{Pb}/\text{Mg} = 1:1$ conditions by mechanical ball milling at 400 rpm for 1 h. Contrary to the conventional solution method, dolomite analogs were successfully synthesized in a short time without the excess addition of Mg amount, which challenges the high Mg theory often considered in dolomite formation and provides new choices for the formation of dolomite. At the same time, milling operation allowed the synthesis of dolomite analogs without the need for controlling the amount of water, different from the oft-claimed constraining roles of strong water and Mg^{2+} influence. Milling operation also enabled the synthesis of the Ca-Mg dolomite phase, although not a pure phase, by avoiding calcite as a barrier. Comparing the differences between the synthesis processes of norsethite, $\text{PbMg}(\text{CO}_3)_2$ and dolomite, it was concluded that the key factor governing the difficulty of dolomite formation is the size of the ionic radius of the A-site elements. The large ionic radius of Ba elements may accommodate the incompletely dehydrated Mg^{2+} to overcome the kinetic hindrance of Mg ion dehydration. The findings reported in this paper provide new insights into the formation pathways of dolomite analogs and even dolomite.

Author Contributions: T.J.: investigation, formal analysis, data curation, writing-original draft preparation, funding acquisition, writing-review and editing; C.W.: methodology, validation, formal analysis, project administration, visualization, writing-review and editing; M.C.: investigation, funding acquisition; H.H.: investigation and software; J.H.: investigation and software; X.C.: investigation and software; Q.Z.: conceptualization, resources, supervision, writing-review and editing; All authors have read and agreed to the published version of the manuscript.

Funding: This study was funded by “The Key R&D Program of Hubei Province” (Project NO. 2022BCA083) and “The Fundamental Research funds for Central University” (Project NO. 2022-ZH-B1-05).

Data Availability Statement: Not applicable.

Acknowledgments: This study was financially supported by “The Key R&D Program of Hubei Province” (Project NO. 2022BCA083) and “The Fundamental Research funds for Central University” (Project NO. 2022-ZH-B1-05).

Conflicts of Interest: The authors declare no conflict of interest.

References

1. Arvidson, R.S. *Dolomites: A Volume in Honor of Dolomieu*; Eos, Transactions American Geophysical Union: Washington, DC, USA, 1996.
2. Qing, H.; Qiao, Z.; Zhang, S.; Cosford, J.; Hu, A.; Liang, F.; Wang, Y.; Zheng, J. $\delta^{26}\text{Mg}$ - $\delta^{13}\text{C}$ - $\delta^{18}\text{O}$ systems as geochemical tracers for dolomite recrystallization: A case study of lower Ordovician dolomite from Tarim Basin. *Chem. Geol.* **2023**, *619*, 121302. [[CrossRef](#)]
3. Rodriguez-Blanco, J.D.; Shaw, S.; Benning, L.G. A route for the direct crystallization of dolomite. *Am. Mineral.* **2015**, *100*, 1172–1181. [[CrossRef](#)]
4. Montes-Hernandez, G.; Findling, N.; Renard, F. Dissolution-precipitation reactions controlling fast formation of dolomite under hydrothermal conditions. *Appl. Geochem.* **2016**, *73*, 169–177. [[CrossRef](#)]
5. Land, L.S. Failure to Precipitate Dolomite at 25 °C from dilute solution despite 1000-fold Oversaturation after 32 Years. *Aquat. Geochem.* **1998**, *4*, 361–368. [[CrossRef](#)]
6. Kell-Duivesteyn, I.J.; Baldermann, A.; Mavromatis, V.; Dietzel, M. Controls of temperature, alkalinity and calcium carbonate reactant on the evolution of dolomite and magnesite stoichiometry and dolomite cation ordering degree; an experimental approach. *Chem. Geol.* **2019**, *529*, 119292. [[CrossRef](#)]
7. Warren, J. Dolomite: Occurrence, evolution and economically important associations. *Earth-Sci. Rev.* **2000**, *52*, 1–81. [[CrossRef](#)]
8. Hardie, L.A. Dolomitization; a critical view of some current views. *J. Sediment. Res.* **1987**, *57*, 166–183. [[CrossRef](#)]
9. Liu, D.; Xu, Y.; Papineau, D.; Yu, N.; Fan, Q.; Qiu, X.; Wang, H. Experimental evidence for abiogenic formation of low-temperature proto-dolomite facilitated by clay minerals. *Geochim. Et Cosmochim. Acta* **2019**, *247*, 83–95. [[CrossRef](#)]
10. Wang, X. Equilibrium between dolomitization and dedolomitization of a global set of surface water samples: A new theoretical insight on the dolomite inorganic formation mechanism. *Mar. Chem.* **2021**, *235*, 104017. [[CrossRef](#)]
11. Pina, C.M.; Pimentel, C.; Crespo, A. The Dolomite Problem: A Matter of Time. *ACS Earth Space Chem.* **2022**, *6*, 1468–1471. [[CrossRef](#)]
12. Lu, F.; Tan, X.; Xiao, D.; Shi, K.; Li, M.; Zhang, Y.; Zheng, H.; Dong, Y. Sedimentary control on diagenetic paths of dolomite reservoirs in volcanic setting: A case study of Permian Chihhsia Formation in Sichuan Basin, China. *Sediment. Geol.* **2023**, *454*, 106451. [[CrossRef](#)]
13. Lu, F.; Tan, X.; Zhong, Y.; Luo, B.; Zhang, B.; Zhang, Y.; Li, M.; Xiao, D.; Wang, X.; Zeng, W. Origin of the penecontemporaneous sucrosic dolomite in the Permian Qixia Formation, northwestern Sichuan Basin, SW China. *Pet. Explor. Dev. Online* **2020**, *47*, 1218–1234. [[CrossRef](#)]
14. Zhang, F.; Yan, C.; Teng, H.H.; Roden, E.E.; Xu, H. In situ AFM observations of Ca–Mg carbonate crystallization catalyzed by dissolved sulfide: Implications for sedimentary dolomite formation. *Geochim. Et Cosmochim. Acta* **2013**, *105*, 44–55. [[CrossRef](#)]
15. Mrose, M.E.; Chao, E.C.T.; Fahey, J.J.; Milton, C. Norsethite, $\text{BaMg}(\text{CO}_3)_2$, a new mineral from the green river formation, Wyoming. *Am. Mineral.* **1961**, *46*, 420–429.
16. Chang, L.L.Y. Synthesis of $\text{MBa}(\text{CO}_3)_2$ compounds. *Am. Mineral.* **1964**, *49*, 1142.
17. Lippmann, F. Syntheses of $\text{BaMg}(\text{CO}_3)_2$ (Norsethite) at 20 °C and the Formation of Dolomite in Sediments. In *Recent Developments in Carbonate Sedimentology in Central Europe*; Springer: Berlin/Heidelberg, Germany, 1968; pp. 33–37.
18. Pimentel, C.; Pina, C.M. The formation of the dolomite-analogue norsethite: Reaction pathway and cation ordering. *Geochim. Cosmochim. Acta* **2014**, *142*, 217–223. [[CrossRef](#)]
19. Pimentel, C.; Pina, C.M. Reaction pathways towards the formation of dolomite-analogues at ambient conditions. *Geochim. Cosmochim. Acta* **2016**, *178*, 259–267. [[CrossRef](#)]
20. Zhang, Y.; Yao, Q.; Qian, F.; Zhou, G.; Fu, S. Formation pathway of norsethite dominated by solution chemistry under ambient conditions. *Am. Mineral.* **2021**, *106*, 1306–1318. [[CrossRef](#)]

21. Boldyrev, V.V. Mechanochemistry and mechanical activation of solids. *Russ. Chem. Rev.* **2006**, *75*, 177–189. [[CrossRef](#)]
22. Baláž, P.; Achimovičová, M.; Baláž, M.; Billík, P.; Cherkezova-Zheleva, Z.; Criado, J.M.; Delogu, F.; Dutková, E.; Gaffet, E.; Gotor, F.J.; et al. Hallmarks of mechanochemistry: From nanoparticles to technology. *Chem. Soc. Rev.* **2013**, *42*, 7571–7637. [[CrossRef](#)]
23. Longo, J.M.; Voight, K.C. Synthesis of mixed-metal carbonates by grinding. *Solid State Ion.* **1989**, *32*, 409–412. [[CrossRef](#)]
24. Gammage, R.B.A.; Glasson, D.R.B.; Hodgson, I.R.B.; O'Neill, P. Microcrystalline structure of milled dolomite and its constituent carbonates. *J. Colloid Interface Sci.* **1983**, *92*, 530–544. [[CrossRef](#)]
25. Radha, A.V.; Fernandez-Martinez, A.; Hu, Y.; Jun, Y.; Waychunas, G.A.; Navrotsky, A. Energetic and structural studies of amorphous $\text{Ca}_{1-x}\text{Mg}_x\text{CO}_3 \cdot n\text{H}_2\text{O}$ ($0 \leq x \leq 1$). *Geochim. Et Cosmochim. Acta* **2012**, *90*, 83–95. [[CrossRef](#)]
26. Xu, J.; Yan, C.; Zhang, F.; Konishi, H.; Xu, H.; Teng, H.H. Testing the cation-hydration effect on the crystallization of Ca-Mg- CO_3 systems. *Proc. Natl. Acad. Sci. USA* **2013**, *110*, 17750–17755. [[CrossRef](#)]
27. Lindner, M.; Saldi, G.D.; Carrocci, S.; Bénézeth, P.; Schott, J.; Jordan, G. On the growth of anhydrous Mg-bearing carbonates—Implications from norsethite growth kinetics. *Geochim. Et Cosmochim. Acta* **2018**, *238*, 424–437. [[CrossRef](#)]
28. Dong, C.; Li, J.; Sun, Z. Synthesis and Transformation of Cerussite and Hydrocerussite. *J. Univ. Jinan* **2012**, *26*, 73–77.
29. Liu, Z.T.Y.; Burton, B.P.; Khare, S.V.; Sarin, P. First-principles phase diagram calculations for the carbonate quasibinary systems CaCO_3 - ZnCO_3 , CdCO_3 - ZnCO_3 , CaCO_3 - CdCO_3 and MgCO_3 - ZnCO_3 . *Chem. Geol.* **2016**, *443*, 137–145. [[CrossRef](#)]
30. Pimentel, C.; Pina, C.M.; Sainz-Díaz, C.I. New Insights into Dolomite and Dolomite-Analogue Structures from First Principles Calculations. *ACS Earth Space Chem.* **2022**, *6*, 2360–2367. [[CrossRef](#)]
31. Böttcher, M.E.; Gehlken, P.L.; Skogby, H.; Reutel, C. The vibrational spectra of $\text{BaMg}(\text{CO}_3)_2$ (norsethite). *Mineral. Mag.* **1997**, *61*, 249–256. [[CrossRef](#)]
32. Hu, H.; Zhang, Q.; Yuan, W.; Li, Z.; Zhao, Y.; Gu, W. Efficient Pb removal through the formations of (basic) carbonate precipitates from different sources during wet stirred ball milling with CaCO_3 . *Sci. Total Environ.* **2019**, *664*, 53–59. [[CrossRef](#)]
33. Li, X.; Zhang, Q.; Yang, B. Co-precipitation with CaCO_3 to remove heavy metals and significantly reduce the moisture content of filter residue. *Chemosphere* **2020**, *239*, 124660. [[CrossRef](#)] [[PubMed](#)]
34. Zeng, C.; Hu, H.; Feng, X.; Wang, K.; Zhang, Q. Activating CaCO_3 to enhance lead removal from lead-zinc solution to serve as green technology for the purification of mine tailings. *Chemosphere* **2020**, *249*, 126227. [[CrossRef](#)] [[PubMed](#)]
35. Zeng, C.; Hu, H.; Feng, X.; Chen, M.; Shi, Q.; Chen, M.; Zhang, Q. Efficient removal of lead impurity for the purification and recycling of nickel from secondary sources based on ball-milling activated CaCO_3 . *J. Environ. Chem. Eng.* **2021**, *9*, 106737. [[CrossRef](#)]
36. Pina, C.M.; Pimentel, C.; García-Merino, M. High resolution imaging of the dolomite (104) cleavage surface by atomic force microscopy. *Surf. Sci.* **2010**, *604*, 1877–1881. [[CrossRef](#)]
37. Cai, W.K.; Liu, J.H.; Zhou, C.H.; Keeling, J.; Glasmacher, U.A. Structure, genesis and resources efficiency of dolomite: New insights and remaining enigmas. *Chem. Geol.* **2021**, *573*, 120191. [[CrossRef](#)]
38. Lippmann, F. Die Kristallstruktur des Norsethit, $\text{BaMg}(\text{CO}_3)_2$, im Vergleich zum Dolomit, $\text{CaMg}(\text{CO}_3)_2$. *Naturwissenschaften* **1967**, *54*, 514. [[CrossRef](#)]

Disclaimer/Publisher's Note: The statements, opinions and data contained in all publications are solely those of the individual author(s) and contributor(s) and not of MDPI and/or the editor(s). MDPI and/or the editor(s) disclaim responsibility for any injury to people or property resulting from any ideas, methods, instructions or products referred to in the content.